IAI
Journals.ASM.org

Hypoxia-Mediated Impairment of the Mitochondrial Respiratory Chain Inhibits the Bactericidal Activity of Macrophages

Melanie Wiese,[a] Roman G. Gerlach,[c] Isabel Popp,[a] Jasmin Matuszak,[a] Mousumi Mahapatro,[a] Kirstin Castiglione,[a] Dipshikha Chakravortty,[e] Carsten Willam,[b] Michael Hensel,[d] Christian Bogdan,[a] and Jonathan Jantsch[a]

Microbiology Institute–Clinical Microbiology, Immunology, and Hygiene[a] and Department of Nephrology and Hypertension,[b] University Hospital of Erlangen and Friedrich-Alexander University, Erlangen-Nuremberg, Germany; Junior Research Group 3, Robert Koch Institute, Wernigerode, Germany[c]; Department of Microbiology, University of Osnabrueck, Osnabrueck, Germany[d]; and Department of Microbiology and Cell Biology, Centre for Infectious Disease Research and Biosafety Laboratories, Indian Institute of Science, Bangalore, India[e]

In infected tissues oxygen tensions are low. As innate immune cells have to operate under these conditions, we analyzed the ability of macrophages (Mϕ) to kill *Escherichia coli* or *Staphylococcus aureus* in a hypoxic microenvironment. Oxygen restriction did not promote intracellular bacterial growth but did impair the bactericidal activity of the host cells against both pathogens. This correlated with a decreased production of reactive oxygen intermediates (ROI) and reactive nitrogen intermediates. Experiments with phagocyte NADPH oxidase (PHOX) and inducible NO synthase (NOS2) double-deficient Mϕ revealed that in *E. coli*- or *S. aureus*-infected cells the reduced antibacterial activity during hypoxia was either entirely or partially independent of the diminished PHOX and NOS2 activity. Hypoxia impaired the mitochondrial activity of infected Mϕ. Inhibition of the mitochondrial respiratory chain activity during normoxia (using rotenone or antimycin A) completely or partially mimicked the defective antibacterial activity observed in hypoxic *E. coli*- or *S. aureus*-infected wild-type Mϕ, respectively. Accordingly, inhibition of the respiratory chain of *S. aureus*-infected, normoxic PHOX$^{-/-}$ NOS2$^{-/-}$ Mϕ further raised the bacterial burden of the cells, which reached the level measured in hypoxic PHOX$^{-/-}$ NOS2$^{-/-}$ Mϕ cultures. Our data demonstrate that the reduced killing of *S. aureus* or *E. coli* during hypoxia is not simply due to a lack of PHOX and NOS2 activity but partially or completely results from an impaired mitochondrial antibacterial effector function. Since pharmacological inhibition of the respiratory chain raised the generation of ROI but nevertheless phenocopied the effect of hypoxia, ROI can be excluded as the mechanism underlying the antimicrobial activity of mitochondria.

Although the content of oxygen in inhaled air is ca. 20%, the physiologic oxygen levels encountered by cells *in vivo* are rarely above 12% O_2 and are, for the most part, between 3 to 5% O_2 (12, 13, 45, 77). Certain layers of the skin as well as cells from the epithelial lining may even encounter oxygen tensions below 3 to 5% under physiological conditions (40, 58). In pathologically altered tissues, in contrast, the oxygen tensions may drop to values well below 2%. In order to avoid nomenclatural confusion, Herzenberg and coworkers suggested use of the term "hypoxic environment" for oxygen tensions below 2% O_2 and the term "physiological oxygen level" for oxygen tensions between 2 and 12% O_2 (5).

Well-established pathological factors leading to severe tissue hypoxia include cancer and ischemia (55, 63, 74, 76). Furthermore, infections in a living organism are frequently associated with very low oxygen tensions in the afflicted tissues (32, 56, 65, 71). This raises the possibility that hypoxia may alter the ability of the immune system to combat the invading pathogen.

Paul Ehrlich hypothesized in 1885 that "the protoplasm (of the host cell), in its avidity for oxygen, may cut off the oxygen supply of the bacteria and [. . .] thus remove the essential factor of their life" (22). Nevertheless, to the best of our knowledge, no detailed studies have been performed in macrophages (Mϕ) in order to confirm or refute this hypothesis. However, there are several lines of evidence suggesting that hypoxia may negatively or positively affect the ability of the host to control infections. Supporting the notion that hypoxia may favor the host's ability to clear off invading pathogens, hypoxia was found to increase the production of the antimicrobial peptide cathelicidin in mouse blood leukocytes (60) and, in the presence of Toll-like receptor (TLR)-dependent stimulation, to upregulate the expression of inducible nitric oxide synthase (iNOS or NOS2) in Mϕ (54) in a hypoxia-inducible factor 1α (HIF1α or HIF1A)-dependent manner. The transcription factor HIF1A plays a key role in allowing cells to adapt to hypoxic conditions (39). Interestingly, hypoxia increased phagocytosis by the RAW264.7 macrophage-like cell line in a HIF1A-dependent manner (3). Intriguingly, even under normoxic conditions the exposure of Mϕ, dendritic cells, or granulocytes to bacteria or lipopolysaccharide (LPS) led to an accumulation of HIF1A protein comparable to that seen with hypoxic stimulation. Furthermore, under normoxic conditions, inflammatory HIF1A was required for (i) the proinflammatory function of myeloid cells (16, 35, 59), (ii) the gene expression of NOS2 (21, 53), and (iii) the control of infections with group A streptococci (16, 60). By boosting HIF1A activity using a pharmacologic approach, the clinical course of an infection with *Staphylococcus aureus* was improved (86). Together, these data favor the hypothesis that bacterial in-

Received 21 September 2011 **Returned for modification** 21 October 2011
Accepted 28 December 2011
Published ahead of print 17 January 2012
Editor: B. A. McCormick
Address correspondence to Jonathan Jantsch, jonathan.jantsch@uk-erlangen.de.
Supplemental material for this article may be found at http://iai.asm.org/.

doi:10.1128/IAI.05972-11

fections in the presence of hypoxia may boost HIF1A activity and thereby promote the antibacterial capacity of myeloid cells.

However, oxygen deprivation not only augments the accumulation and transcriptional activity of HIF1A but also inhibits the activity of the oxygen-dependent enzymes NOS2 and phagocyte NADPH oxidase (PHOX) (2, 18, 41, 44, 66, 81). Since both enzymes are of paramount importance to controlling certain viral, bacterial, protozoan or fungal infections *in vivo* (8, 9, 75), hypoxia may inhibit the ability of myeloid cells to kill ingested microbes. In lung and skin infection models with *S. aureus* it has been demonstrated that systemic hypoxia inhibits the clearance of *S. aureus* (29, 38). In line with this observation granulocytes showed a reduced ability to kill bacteria (including *S. aureus* and *Escherichia coli*) under hypoxic conditions (49). However, to the best of our knowledge, the ability of primary Mϕ to kill bacteria under hypoxic conditions has not yet been studied. Furthermore, there are no reports on comparative analyzes of the possible mechanisms by which hypoxia might impair the bactericidal activity of myeloid cells.

In the present study we tested whether a reduced oxygen supply affects the ability of Mϕ to kill Gram-negative (*E. coli*) or Gram-positive (*S. aureus*) bacteria. We found that under hypoxic conditions Mϕ are impaired to kill both pathogens. Unexpectedly, this defective antibacterial activity could not be solely attributed to a reduced activity of PHOX or NOS2, but also resulted from an inhibition of the mitochondrial respiratory function during hypoxia.

MATERIALS AND METHODS

Mouse strains. C57BL/6 wild-type (WT) mice were purchased from Charles River Breeding Laboratories (Sulzfeld, Germany). Breeding pairs of *Cybb*$^{-/-}$ *Nos2*$^{-/-}$ mice were kindly provided by W.-D. Hardt (ETH Zurich, Switzerland), where *Cybb* represents cytochrome *b*-245 beta chain (gp91^{phox}). *Cybb*$^{-/-}$ *Nos2*$^{-/-}$ mice were generated by crossing B6.129S6-*Cybbtm1Din*/J40 mice and B6;129P2-*Nos2tm1Lau*/J41 mice (both from Jackson Laboratory) as described by Ackermann et al. (1). The *Cybb*$^{-/-}$ *Nos2*$^{-/-}$ mice were bred at the Franz-Penzoldt Animal Center of the Friedrich-Alexander-University Erlangen-Nürnberg. All mice were kept under specific-pathogen-free conditions.

Preparation of Mϕ. Mϕ were grown from bone marrow tissues of C57BL/6 WT and *Cybb*$^{-/-}$ *Nos2*$^{-/-}$ mice as described previously (85). To control the purity of bone marrow (BM)-derived Mϕ, the cells were subjected to flow cytometry (FACSCalibur; BD Biosciences, Heidelberg, Germany) after surface staining with fluorochrome-labeled antibodies (all from BD Biosciences, unless otherwise stated): anti-CD11b (clone M1/70) and anti-F4/80 (clone CI:A3; Serotec, Düsseldorf, Germany). The specificity of the stainings was verified by the use of isotype control monoclonal antibodies. At day 7 of BM culture, Mϕ were harvested and routinely yielded a population of >90% CD11b^{high} F4/80^{high} Mϕ. The cells were allowed to settle for at least 2 h in conventional polystyrene plates (Greiner Bio One, Frickenhausen, Germany; Corning Costar, Amsterdam, Netherlands). Where indicated, the cells were seeded in gas-permeable plates (Lumox Multiwell; Sarstedt, Nürnbrecht, Germany) or low-attachment plates (Corning, Wiesbaden, Germany).

Bacterial strains and growth conditions. *E. coli* strain HB101 and *S. aureus* strain ATCC 25923 were used to infect Mϕ. All bacteria were routinely grown in Luria-Bertani (LB) broth or on Mueller-Hinton plates at 37°C. Plasmid pDiGc was kindly provided by David Holden, London, United Kingdom. The *E. coli* strain harboring the pDiGc plasmid was grown in LB supplemented with carbenicillin (50 μg/ml) or LB broth containing 0.2% arabinose where indicated.

Bacterial infection of Mϕ. Mϕ were infected with *E. coli* HB101 or *S. aureus* ATCC 25293 grown to stationary phase. The concentrations of the bacterial suspensions were adjusted by reading the optical density at 600 nm (OD_{600}). The actual multiplicity of infection (MOI) of each experiment was assessed by plating dilutions of the infection inocula onto agar plates for the determination of the number of CFU. For synchronization of infection, centrifugation at 1,400 rpm for 5 min was performed. Mϕ were infected at an MOI of 10 for 60 min at 37°C in 5% CO_2. After infection, the cells were washed twice with phosphate-buffered saline (PBS) to remove noninternalized bacteria. To kill the residual extracellular bacteria, the cells were treated with RPMI 1640 medium supplemented with 10% fetal calf serum, 0.05 mmol of 2-mercaptoethanol (2-ME)/liter, and 10 mM HEPES containing gentamicin at a concentration of 100 μg/ml for 1 h, followed by treatment with 25 μg of gentamicin/ml for the rest of the experiment. Two hours after infection, the cells were cultured under normoxic conditions in a regular humidified incubator (37°C, 5% CO_2, 21% O_2) or under hypoxic conditions (37°C, 5% CO_2, 0.5% O_2) using an adjustable hypoxic humidified workbench suitable for cell culture experiments (invivo300; Ruskinn Technology, West Yorkshire, United Kingdom). To examine the influence of reoxygenation, the cells were first incubated for 8 h under hypoxic conditions and then kept under normoxic conditions for the rest of the experiment. Where indicated, rotenone dissolved in chloroform (R8875 [Sigma-Aldrich, Deisenhofen, Germany], with a 100 mM concentration of stock solution) or antimycin A dissolved in 100% ethanol (A8674 [Sigma-Aldrich], with a 50-mg/ml concentration of stock solution) was added at a final concentration of 100 μM (rotenone) or 4 μg/ml (antimycin A) 2 h after infection. In these experiments, cells incubated with the respective concentrations of chloroform or ethanol alone served as controls.

Cells were lysed 2 and 24 h after infection using 0.1% Triton X-100 in PBS to recover intracellular bacteria. The number of intracellular bacteria was determined by serial 10-fold dilutions in 0.05% Tween 80 in PBS and subsequent plating on a Mueller-Hinton (MH) agar plate to enumerate the CFU. The killing rate of myeloid cells is given as a percentage of the surviving bacteria and was calculated as follows: (average CFU at 24 h/average CFU at 2 h) $\times$ 100.

Monitoring of the growth of *E. coli* and *S. aureus* in LB media. The proliferative behavior of *E. coli* and *S. aureus* under both normoxic and hypoxic conditions was investigated by monitoring the growth of a diluted bacterial suspension. An overnight bacterial culture was diluted in LB or cell culture medium in the same way as it was done for the infection of Mϕ (see above). The bacteria were incubated under normoxic or hypoxic conditions. To investigate the effect of rotenone and antimycin A, each was added to the growth medium at a final concentration of 100 μM (rotenone) and 4 μg/ml (antimycin A). At different time points, the CFU/ml of each sample was determined by plating serial dilutions of an aliquot of the bacterial suspension on MH agar plates.

Fluorescence dilution assays to detect the proliferation of intracellular bacteria. To monitor the proliferative activity of intracellular *E. coli*, Mϕ were infected with an *E. coli* HB101 strain harboring a dual fluorescence reporter plasmid (pDIGc) (31). This strain shows a constitutive expression of green fluorescent protein (GFP), whereas the expression of the DsRed protein (red fluorescent protein) is arabinose inducible. Therefore, the growth of the bacteria can be monitored by measuring the fluorescence intensity of DsRed after transferring an arabinose-induced bacterial suspension to arabinose-free conditions. The GFP expression was used to identify the bacteria during flow cytometric analysis. *E. coli* HB101 pDiGc strain was grown overnight in LB broth containing 0.2% arabinose. Prior to infection, the bacteria were washed twice with PBS, and all further steps were performed under arabinose-free conditions. At different time points after infection, the cells were lysed with 0.1% PBS–Triton X-100, and the DsRed fluorescence intensity of GFP-positive bacterium-sized particles was measured via flow cytometry (DsRed, FL-2; GFP, FL-1 [10,000 events in the FL-1 gate]). As a control, the same amount of bacteria used to infect the Mϕ was incubated in cell culture medium for 6 h under normoxic and hypoxic conditions. As expected, an increase in bacterial counts was accompanied by a dilution of DsRed fluorescence in the GFP-positive fraction under both conditions.

To analyze the replication dynamics of intracellular *S. aureus*, the bacteria

were stained prior to infection with carboxyfluorescein diacetate (CFDA) succinimidyl ester (CFSE) mixed isomers (C1157; Invitrogen, Carlsbad, CA). To this end, 500 μl of an overnight grown *S. aureus* culture was washed twice with PBS and incubated with PBS containing 5 μM CFSE for 15 min at 37°C in the dark. Afterwards, the bacteria were washed twice with ice-cold PBS containing 5% fetal calf serum (FCS) and then resuspended in cold PBS. The cells were infected as described above using the CFSE-stained *S. aureus*. At the indicated time points, the infected Mϕ were lysed with PBS–0.1% Triton X-100. To distinguish between cell debris and bacteria, the lysates were stained with an *S. aureus*-specific antibody (AP00865PU-N, 1:100 rabbit anti-*S. aureus* [Acris Antibodies, Herford, Germany]) in PBS containing 1% bovine serum albumin (BSA) and 10% FCS for 1 h at 4°C. After incubation of the lysates with a goat anti-rabbit IgG (H+L) Alexa Fluor 647-coupled secondary antibody (A21245; Invitrogen), diluted 1:500 in PBS containing 1% BSA and 10% FCS for 1 h at 4°C in the dark, the CFSE fluorescence intensity of Alexa Fluor 647-positive bacterial particles was analyzed by flow cytometry (CFSE, FL-1; Alexa Fluor 647, FL-4 [10,000 events in the FL-4 gate]). As a control, the same amount of bacteria that was used for infecting Mϕ was incubated in cell culture medium for 6 h under normoxic and hypoxic conditions. As expected, an increase in bacterial counts was accompanied by a dilution of CFSE fluorescence in the Alexa Fluor 647-positive fraction under both conditions.

siRNA duplexes. Nonsilencing small interfering RNA (ns-siRNA) duplexes (catalog no.1027281 [Qiagen, Hilden, Germany]) were directed against the following nonsense target sequence: AATTCTCCGAACGTG TCACGT (sense, UUCUCCGAACGUGUCACGUdTdT; antisense, ACG UGACACGUUCGGAGAAdTdT). *Hif1a*-specific, silencing siRNA molecules were obtained from Dharmacon's prevalidated siRNA database (*Hif1a*-specific, prevalidated siRNA; catalog no. L040638). The duplexes were dissolved in siRNA suspension buffer (Qiagen) to a final concentration of 0.3 μg/μl (20 μM), heated for 1 min to 90°C, and incubated at 37°C for 60 min. Resolved duplexes were stored in aliquots at −80°C.

RNA interference studies. RNA interference was performed as described previously (35, 36, 85). Mϕ were harvested, washed four times with Opti-MEM (Invitrogen), and resuspended at a concentration of 4×10^7 cells/ml. Then, 20-μl portions of a 20 μM solution of the respective siRNA duplexes were transferred to a 4-mm cuvette (Peqlab, Erlangen, Germany), and the final volume was adjusted to 50 μl with Opti-MEM. A total of 50 μl of the cell suspension (containing 2×10^6 cells) was added and pulsed in a Gene Pulser Xcell apparatus (Bio-Rad). The pulse conditions were 400 V, 150 μF, and 100 Ω. After electroporation, the cells were transferred into serum-free RPMI 1640 cell culture medium. After 1 h, an equal amount of RPMI 1640 medium supplemented with 20% FCS was added. After 24 h, electroporated Mϕ were infected as described above.

RNA extraction and cDNA synthesis. At various time points, total RNA was isolated by phenol-chloroform extraction using Trifast (Peqlab) according to the manufacturer's instructions. Briefly, the cells were washed with PBS and rinsed off the plate with Trifast. The phenolic suspension was mixed with a 1/5 volume of chloroform and centrifuged for 15 min at 12,000 × g and 4°C. The upper, aqueous phase was transferred into a new reaction tube. By adding 1 volume of isopropanol and incubating the sample for 10 min at room temperature, the RNA was precipitated and pelleted by centrifugation (12,000 × *g*) at 4°C for 15 min. After the pellet was washed with 75% ethanol, the RNA was resuspended in RNase-free water and incubated at 60°C for 10 min. Then, 1 to 2 μg of total RNA was reverse transcribed using a high-capacity cDNA archive kit (Applied Biosystems, Darmstadt, Germany).

Real-time PCR. After RNA extraction and cDNA synthesis, real-time PCR was performed using an ABI Prism 7900 sequence detector (Applied Biosystems) with TaqMan Universal Mastermix and Assays-on-Demand (Applied Biosystems), which include forward and reverse primers and the FAM-labeled probe for the target gene, respectively. The following assays were used: murine hypoxanthine guanine phosphoribosyl transferase 1 (*Hprt1*; Mm00446968_m1), phosphoglycerate kinase 1 (*Pgk1*; Mm01225301_m1), and *Hif1a* (Mm01283760). Each cDNA was amplified and measured in duplicates or triplicates with 50 to 100 ng of cDNA/well in a reaction volume of 15 μl and the following cycle conditions: 2 min at 50°C, 10 min at 95°C, and then 15 s at 95°C and 60 s at 60°C for 40 cycles. mRNA levels were calculated using SDS 2.1 software (Applied Biosystems). The amount of mRNA for each gene was normalized to the housekeeping gene *Hprt1*.

Detection of reactive nitrogen intermediates (RNI). The production of reactive nitrogen species was investigated by measuring the nitrite accumulation of Mϕ 24 h after infection by the Griess reaction using sodium nitrite as a standard (20).

Measurement of intracellular ROI using CM-H_2DCFDA. For the detection of intracellular reactive oxygen intermediates (ROI), Mϕ were infected as described above. After 24 h, the cells were stained with CM-H_2DCFDA [5-(and 6)-chloromethyl-2′,7′-dichlorodihydrofluorescein diacetate, acetyl ester; Invitrogen], a fluorescent dye that shows a higher fluorescence intensity when reacting with intracellular ROI. To avoid reoxygenation of the hypoxic samples, all staining steps were performed in the hypoxia chamber, and all buffers and reagents were equilibrated for at least 6 h to hypoxic conditions. After the cells were washed twice with PBS, the Mϕ were loaded with ROI-sensitive dye by incubation in PBS containing 20 μM CM-H_2DCFDA for 15 min at 37°C and 5% CO_2 under hypoxic or normoxic conditions. Loading of the cells was stopped by two washes with PBS. The cells were then covered with RPMI 1640 culture medium containing 10% FCS, 0.05 mM 2-ME, and 10 mM HEPES and placed for 15 min at 37°C, 5% CO_2, and either normoxia or hypoxia. As a positive control, some of the cells were treated with phorbol myristate acetate (100 ng/ml) for the final 15 min. The samples were fixed with 3.5% paraformaldehyde (PFA), and the CM-H_2DCFDA fluorescence intensity of whole cells was analyzed by flow cytometry (10,000 events; FL-1).

Analysis of the mitochondrial membrane potential. Changes in the mitochondrial membrane potential ($\Delta\Psi_M$) were measured using JC-1 dye (JC-1 mitochondrial membrane potential assay; Biomol, Hamburg, Germany). A total of 100,000 macrophages were seeded in a black-pigmented, flat-bottom 96-well plate with a transparent bottom (Brand Plates, Wertheim, Germany). Mϕ were infected as described above and subjected to hypoxia or treated with 100 μM rotenone. At least 24 h after infection, JC-1 staining was performed according to the manufacturer's instructions in 100 μl of medium under the respective pO_2. Briefly, 10 μl of JC-1 staining solution was added to the cells for 15 min. The cells were washed twice with the assay buffer; finally, 100 μl of assay buffer was added, and the 96-well plate was sealed with an adhesive clear seal suitable for quantitative (real-time) reverse transcriptase PCR (qRT-PCR) applications (4titude, Wotton, United Kingdom) in order to preserve the respective atmospheric condition. Immediately thereafter, the fluorescence was read at an excitation of 485 nm and an emission of 538 nm (green) and at an excitation of 530 nm and an emission of 590 nm (red) in a Fluoroskan Ascent FL microplate fluorescent reader (Labsystems, Frankfurt, Germany). The ratio of red to green was calculated and is given as the $\Delta\Psi_M$ in arbitrary units.

Immunoblotting. At the indicated time points, Mϕ cell monolayers were lysed using a PE lysis buffer (6.65 M urea, 10% glycerin, 1% sodium dodecyl sulfate [SDS], 10 mM Tris-HCl [pH 6.8], 5 mM dithiothreitol) in the presence of a protease inhibitor cocktail (Roche Diagnostics, Mannheim, Germany). Lysates were diluted with SDS-PAGE sample buffer. Then, 60 μg of protein was separated by SDS-PAGE and transferred onto a polyvinylidene difluoride membrane (Millipore, Schwalbach, Germany). NOS2 (iNOS) was detected using an NOS2-specific antibody (U.S. Biologicals, catalog no. N5350-10B.100). Actin was detected by using an actin-specific antibody from Sigma-Aldrich (catalog no. A2066). HIF1A (HIF-1α) was detected by using an HIF1A-specific antibody (Cayman Chemical, Ann Arbor, MI, catalog no. 10006421). HIF2A (HIF-2α) was detected by using an HIF2A-specific antibody (Novus Biologicals, distributed by Acris Antibodies, Germany, catalog no. NB 100-122). Bound antibodies were visualized by using enhanced chemiluminescence technology.

LDH release assay. To analyze the viability of the cells under the certain conditions, the release of the cytosolic lactate dehydrogenase (LDH)

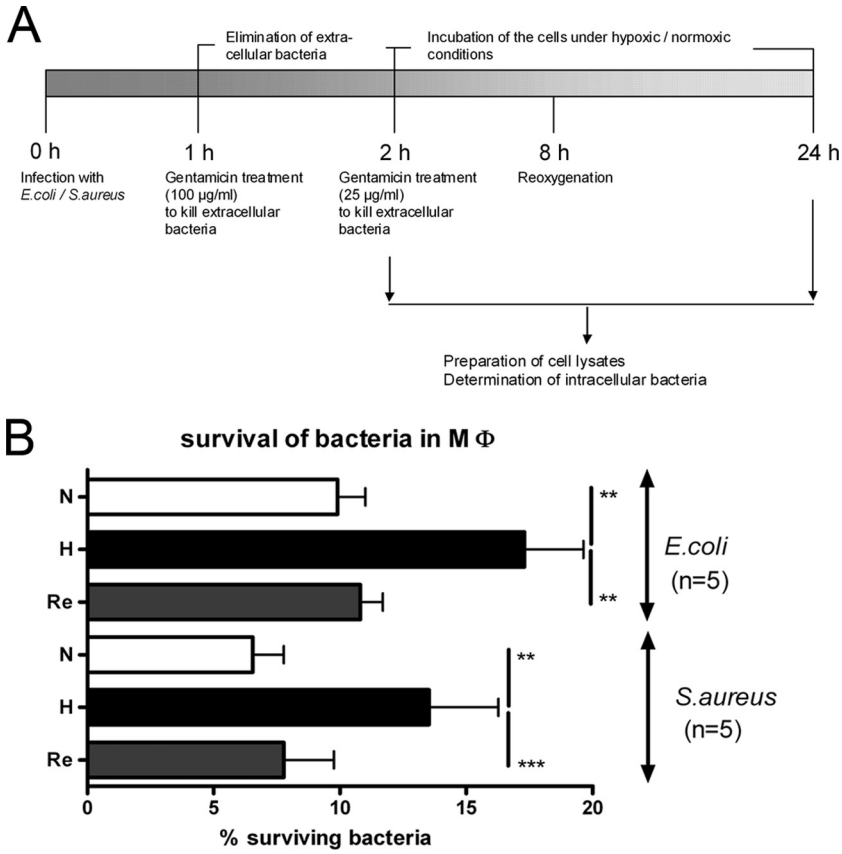

FIG 1 Impaired ability of murine bone marrow-derived macrophages (Mϕ) to kill intracellular bacteria under hypoxic conditions. (A) Schematic representation of the experimental setup for assaying intracellular survival of *E. coli* and *S. aureus* under normoxic and hypoxic conditions. Mϕ were infected with either *E. coli* or *S. aureus* at an MOI of 10. One hour after infection extracellular bacteria were removed by a wash with PBS, followed by gentamicin treatment. At 2 h after infection the cells were exposed to either normoxia (N) or hypoxia (H; 0.5% oxygen). For reoxygenation (Re) the cells were first incubated for 8 h under hypoxic conditions and then kept in normoxia. Cell lysates were prepared 2 and 24 h after infection to determine the amount of CFU inside the cells. (B) The graphs shows the percentage of intracellular bacteria in Mϕ under the indicated conditions. Relative survival was calculated by dividing the amount of intracellular bacteria recovered 24 h after infection related to the amount of intracellular bacteria determined 2 h after infection. The data are means + standard errors of the mean (SEM) of five independent experiments. *, $P < 0.05$; **, $P < 0.01$; ***, $P < 0.001$.

was measured. Therefore, the supernatants of the cells were collected 24 h after infection, and the extracellular LDH content was determined by using a cell death detection kit (Roche) according to the manufacturer's instructions. To take into account that an intracellular induction of the LDH expression might lead to an increase in the release of this enzyme, the intracellular LDH activity was also investigated after lysing the cells using 0.1% Triton X-100. To evaluate the relative LDH release, the OD_{492} of the supernatant was divided by the OD_{492} of the cell lysate derived from the same sample. Afterward, the relative LDH release of the control sample (untreated cells under normoxic conditions) was set to 1. Referring to this value, the change in the relative release of LDH was calculated.

Annexin V and propidium iodide assay. Approximately 500,000 cells were stained in 100 μl of 1× annexin V binding buffer (BD Biosciences) with annexin V APC (1:100; BD Biosciences) for 15 min at room temperature in the dark. Immediately before analysis of the cells with a flow cytometer, 1 μg of propidium iodide (Sigma-Aldrich)/ml was added.

Statistical analysis. Statistical analysis was performed using the Student *t* test.

RESULTS

Mϕ are impaired in their ability to kill ingested *S. aureus* and *E. coli* under hypoxic conditions. *S. aureus* and *E. coli* are known to be readily killed by murine Mϕ under normoxic conditions (47, 61). We assumed that directly after a bacterial infection *in vivo* physiological oxygen tensions will prevail, whereas during the progression of the infection the oxygen tension will progressively drop to low levels. In order to mimic this situation *in vitro*, we subjected infected Mϕ to hypoxic conditions from 2 h after infection with *E. coli* HB101 or *S. aureus* onward until the time point of readout (24 h after infection) (Fig. 1A). Under hypoxic conditions we recovered more bacteria from Mϕ than under normoxic conditions (Fig. 1B; see also Table S1 in the supplemental material). However, the amount of intracellular bacteria retrieved from cells that had been exposed to hypoxia for 8 h and then subjected to normoxic conditions for 16 h (reoxygenation) was indistinguishable from infected cells that had only been cultivated under normoxic conditions (Fig. 1B; see also Table S1 in the supplemental material). This indicates that the effect of hypoxia on the survival of intracellular bacteria is fully reversible.

Hypoxia does not promote the bacterial growth within Mϕ. Next, we wanted to clarify whether the increased survival of *S. aureus* and *E. coli* was due to an increased bacterial proliferation within the host cells under hypoxic conditions or to the impairment of an antibacterial mechanism. Therefore, we analyzed the

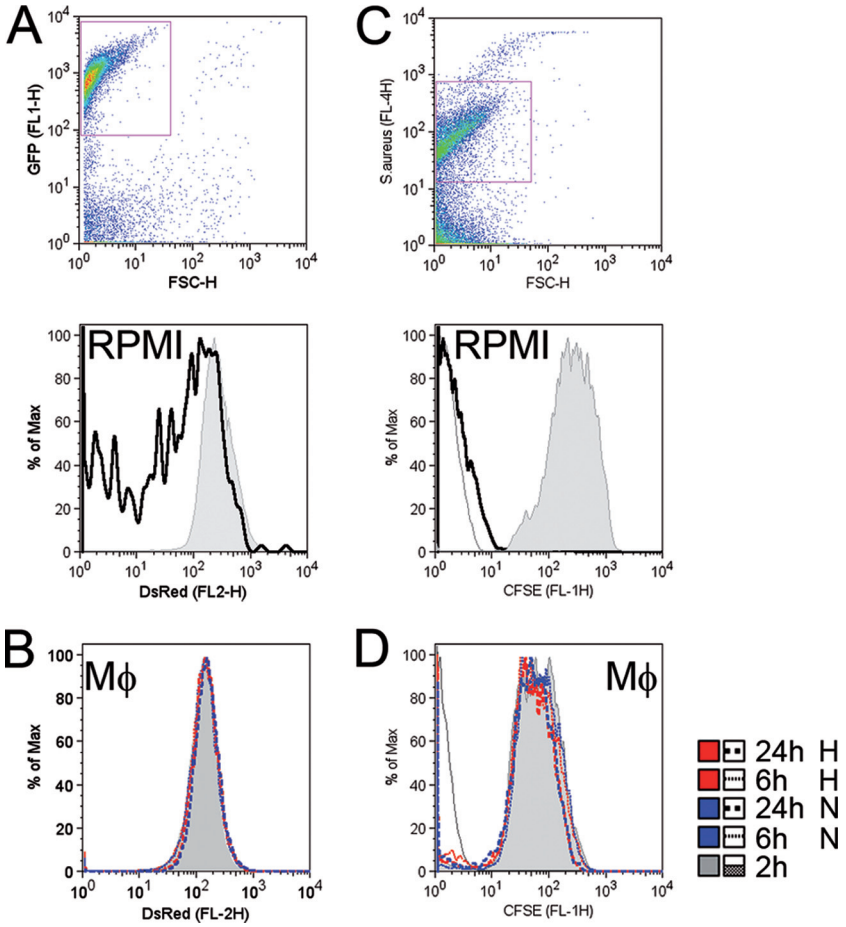

FIG 2 Hypoxia does not improve the bacterial growth within Mϕ. (A and B) To study the replication dynamics of *E. coli*, a strain was used harboring a dual fluorescence reporter plasmid (pDiGc) in which the production of DsRed protein is arabinose inducible, whereas the expression of eGFP is constitutive. The proliferation of bacteria can be monitored by measuring the dilution of DsRed fluorescence after placing the bacterial suspension to arabinose-free conditions. Growing *E. coli* (pDiGc) strains were analyzed immediately (0 h) after placement into arabinose-free medium (RPMI) and 6 h thereafter. (A) GFP-positive, bacterium-sized particles were identified by flow cytometry and in that population the DsRed fluorescence was analyzed. (B) Mϕ were infected with pDiGc-containing *E. coli*. After different time points, the cells were lysed, and the DsRed fluorescence of GFP-positive, bacterium-sized particles was measured by flow cytometry. The results of a representative experiment out of at least two similar experiments are displayed. (C and D) The replication of *S. aureus* was investigated by labeling the bacteria with CFSE. (C) Bacteria were identified after an *S. aureus*-specific staining. The proliferation of CFSE-labeled *S. aureus* in medium (RPMI) was accompanied by a reduction in CFSE fluorescence intensity. (D) Mϕ were infected with CFSE-labeled *S. aureus*. At different time points, the cells were lysed, the bacteria were identified by *S. aureus*-specific staining, and *S. aureus*-positive, bacterium-sized particles were analyzed for CFSE fluorescence. The results of a representative experiment out of at least two similar experiments are displayed.

bacterial growth of *E. coli* and *S. aureus* grown under normoxic and hypoxic conditions in LB broth. Hypoxia did not increase the growth of *E. coli* or *S. aureus* compared to normoxic conditions (see Fig. S1 in the supplemental material). Next, we analyzed the intracellular replication dynamics of *E. coli* and *S. aureus* in Mϕ. To this end, we used (i) an *E. coli* strain harboring a reporter plasmid (pDiGc) and (ii) CFSE-labeled *S. aureus*. The dual fluorescence reporter plasmid (pDiGc) encodes a reporter system in which the production of DsRed protein is arabinose inducible, whereas the expression of eGFP is constitutive (31). The proliferation of pDiGc-harboring *E. coli* can be monitored by measuring the dilution of DsRed fluorescence after the bacterial suspension is transferred to arabinose-free conditions for 6 h (Fig. 2A). After labeling of *S. aureus* with CFSE, the replication of *S. aureus* can be assayed by dilution of CFSE-fluorescence for 6 h (Fig. 2C). When Mϕ were infected with pDiGc harboring *E. coli* or CFSE-labeled *S. aureus*, we could not detect a dilution of DsRed or CFSE fluorescence irrespective of whether the infected cells were cultured under normoxic or hypoxic conditions (Fig. 2B and D). Taken together, these findings demonstrate that hypoxia does not promote intracellular bacterial proliferation but impairs the host's antibacterial capacity.

HIF1A accumulation in *S. aureus*-infected Mϕ does not account for the impaired killing of *S. aureus* under hypoxic conditions. HIF1A accumulation has been demonstrated to be a common feature of infected tissues (83) and has been associated with an antibacterial function of myeloid cells (16, 60). Furthermore, it has been shown that macrophages accumulate HIF2A as well and that HIF2A plays an important role in the regulation of Mϕ function (33, 79). Therefore, we analyzed the status of both HIF-α isoforms (HIF1A and HIF2A) in *E. coli*- and *S. aureus*-infected Mϕ.

Infection with either pathogen under normoxic conditions resulted in the accumulation of HIF1A and HIF2A (Fig. 3A). Hypoxic incubation of infected cells did not further induce HIF2A

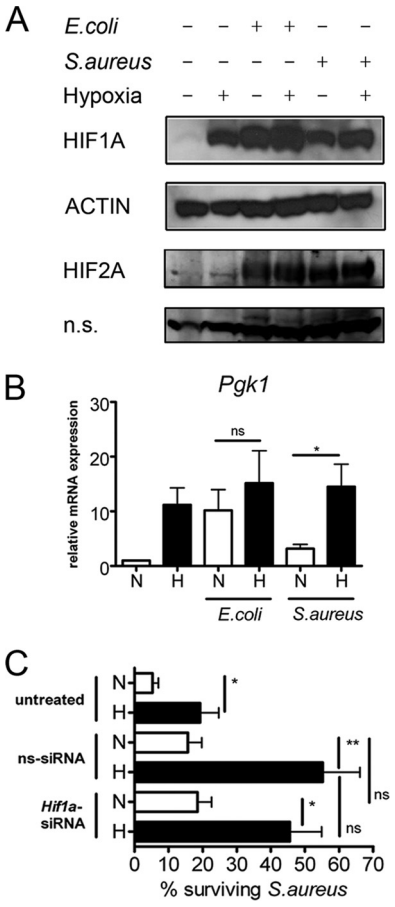

FIG 3 Hypoxia augmented the HIF1A activity of *S. aureus*-infected Mϕ but does not contribute to the impaired killing of *S. aureus* under hypoxic conditions. (A) Cellular lysates were prepared of Mϕ infected with *E. coli* or *S. aureus* under normoxic or hypoxic conditions for 24 h, and immunoblotting for HIF1A and HIF2A was performed. Equal loading is demonstrated in HIF1A immunoblots by incubating the blots with an actin-specific antibody. To demonstrate equal loading in blots probed for HIF2A, a nonspecific band (n.s.) of the HIF2A antibody is shown. The results of a representative experiment out of at least three similar experiments are displayed. (B) Mϕ were infected with *E. coli* or *S. aureus* under normoxic (N) or hypoxic (H) conditions for 24 h, and qRT-PCR was performed with *Pgk1* as the target and *Hprt1* serving as the internal control. The data are means + the SEM of four experiments. *, $P < 0.05$; **, $P < 0.01$; ***, $P < 0.001$. (C) ns-siRNA (ns) or *Hif1a*-specific (*Hif1a*) siRNA was transferred into Mϕ, or the cells were left untreated (untreated). After 24 h, the cells were infected with *S. aureus* and subjected to normoxic (N) or hypoxic (H) conditions. Cell lysates were prepared 2 and 24 h after infection to determine the CFU count inside the cells. The relative survival was calculated by dividing the amount of intracellular bacteria recovered 24 h after infection related to the amount of intracellular bacteria determined 2 h after infection. The data are means + the SEM of four experiments. *, $P < 0.05$; **, $P < 0.01$; ***, $P < 0.001$.

accumulation. Therefore, we conclude that it is very unlikely that HIF2A accounts for the impaired antibacterial capacity under hypoxic conditions.

Under normoxic conditions infection of Mϕ with *E. coli* resulted in a higher HIF1A protein content compared to an infection of Mϕ with *S. aureus*. This resulted in an increased expression of the HIF1A target gene *Pgk1* (Fig. 3A and B). In *S. aureus*-infected cells hypoxia further unregulated the level of HIF1A protein, which was not the case in *E. coli*-infected cells (Fig. 3A). Accordingly, hypoxia increased the expression of the HIF1A target gene *Pgk1* mRNA in *S. aureus* infected Mϕ but not in *E. coli*-infected host cells (Fig. 3B).

Since the impaired antibacterial capacity of the host cells under hypoxic conditions correlated with an increased accumulation of HIF1A in *S. aureus*-infected cells, we investigated whether HIF1A accounts for this hypoxia-induced phenotype using an RNA interference approach. Silencing of *Hif1a* in *S. aureus*-infected Mϕ failed to restore the antibacterial activity under hypoxic conditions (Fig. 3C). As described earlier (35–37), knockdown efficiency was evaluated by analyzing HIF1A protein, *Hif1a* mRNA, and the HIF1A-dependent metabolic target gene *Pgk1* (see Fig. S2 in the supplemental material). There was also no effect of *Hif1a* silencing on the killing of *S. aureus* by normoxic host cells (Fig. 3C). From these data we conclude that the impaired antibacterial capacity of Mϕ under hypoxic conditions is independent of the increased HIF1A accumulation.

Hypoxia abrogates the production of ROI and RNI by Mϕ in response to infection. Since NOS2 and PHOX are oxygen-dependent enzymes (2, 18, 41, 44, 51, 66, 81), we analyzed the production of ROI and RNI in infected Mϕ. As expected, infection of Mϕ with *E. coli* under normoxic conditions induced a robust generation of NO, which was severely impaired in a hypoxic environment. However, if the cells were reoxygenated for 16 h after an initial 8 h period of hypoxia, NO levels reached normoxic levels again (Fig. 4A). Next, we tested whether the impaired NO production under hypoxia results from a reduced NOS2 activity or from a diminished NOS2 protein induction under hypoxic conditions. Infection with *E. coli* led to a comparable NOS2 protein expression under both normoxic and hypoxic conditions, strongly suggesting that hypoxia incapacitates the enzyme activity of NOS2. In contrast to infection with *E. coli*, infection of Mϕ with *S. aureus* hardly caused an induction of NOS2 protein and NO production (Fig. 4A and B).

Next, we quantified the production of ROI by Mϕ using the CM-H_2DCFDA fluorochrome, which is a nonselective detector of various reactive oxygen species. In order to assess the ROI production under hypoxic conditions and to avoid any assay related reoxygenations, we were particularly careful to ensure that the entire staining procedure of the hypoxia-treated samples was performed in the hypoxia chamber and that all buffers and reagents were equilibrated to hypoxic conditions. After loading of the dye and incubation under the respective oxygen tension, the samples were fixed with equilibrated PFA and subjected to flow cytometry. Fixation with PFA neither generated fluorescence signals nor inhibited the fluorescence of CM-H_2DCFDA (data not shown). Under hypoxic conditions we could not detect any production of ROI after infection with *E. coli* and *S. aureus*, whereas ROI were readily detectable under normoxic conditions (Fig. 4C). Together, our data show that hypoxia prevents the production of RNI and ROI in response to a bacterial infection of Mϕ, as expected from the oxygen dependency of NOS2 and PHOX.

A PHOX- and NOS2-independent, oxygen-dependent antimicrobial mechanism contributes to the control of *E. coli* and *S. aureus* in Mϕ. In order to investigate whether the reduced antibacterial capacity of Mϕ during hypoxia simply results from an absent NOS2 and PHOX activity, we infected Mϕ deficient for both NOS2 and PHOX ($Cybb^{-/-}$ $Nos2^{-/-}$) and tested the impact of hypoxia versus normoxia on the survival of *E. coli* or *S. aureus* in these cells. First, we confirmed that a deficiency in NOS2 and

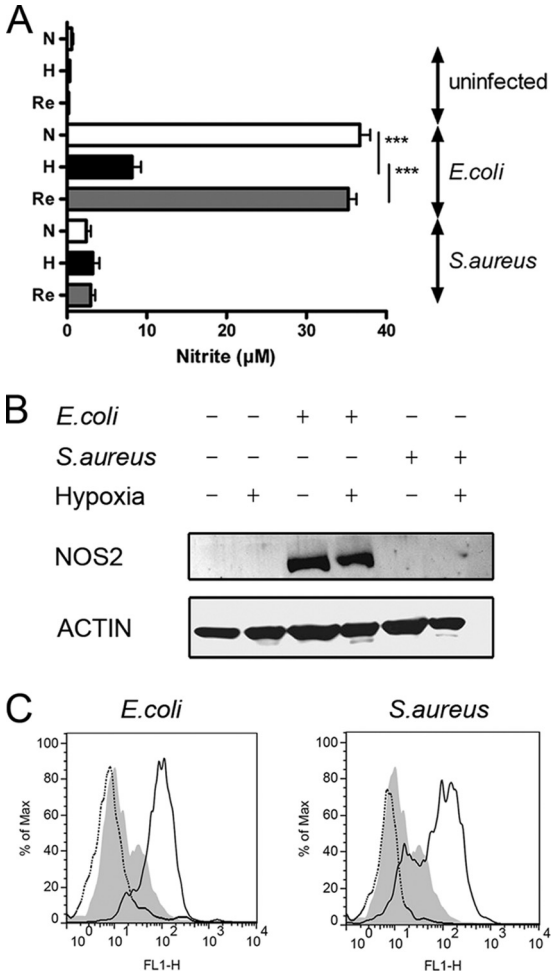

FIG 4 Hypoxia interferes with the production of oxygen radicals and nitrogen production in response to infection of Mϕ. Mϕ were infected with *E. coli* or *S. aureus* at an MOI of 10. One hour after infection, the extracellular bacteria were removed by washing with PBS, followed by gentamicin treatment. At 2 h after infection, the cells were exposed to either normoxia (N) or hypoxia (H; 0.5% oxygen). For reoxygenation (Re), the cells were first incubated for 8 h under hypoxic conditions and then kept in normoxia. (A) After 24 h, the supernatants were collected, and nitrite was measured using the Griess reaction. The data are means + the SEM of five experiments. *, $P < 0.05$; **, $P < 0.01$; ***, $P < 0.001$. (B) Cellular lysates were prepared, and immunoblotting was performed for NOS2 and actin. The results of a representative experiment from at least three similar experiments are shown. (C) Cells were infected as described in panel A. After 24 h, the cells were labeled with CM-H_2DCFDA, fixed with 3.5% PFA, and analyzed by flow cytometry. The gray-shaded curve indicates the FL-1 fluorescence of uninfected labeled cells under normoxic conditions. The dotted black curve indicates the FL-1 fluorescence of CM-H_2DCFDA-labeled cells under hypoxic conditions, and the solid line curve indicates the FL-1 fluorescence of CM-H_2DCFDA-labeled cells under normoxic conditions. The results of a representative experiment out of at least three similar experiments are displayed.

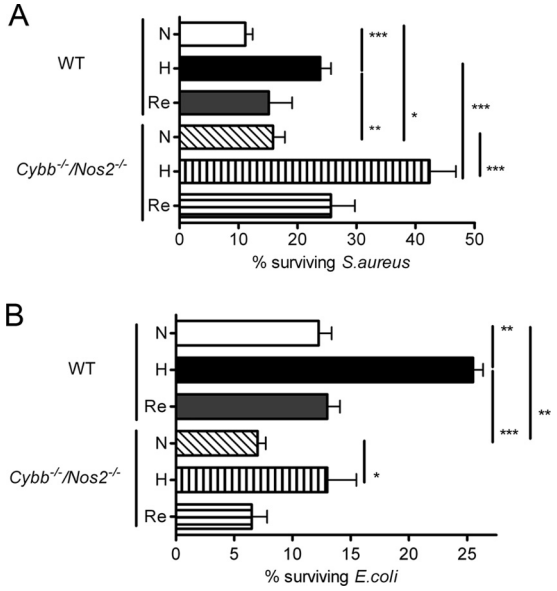

FIG 5 Inhibition of the phagocyte oxidase and NO synthase does not solely explain the impaired killing of *S. aureus* under hypoxic conditions and is not related with the impaired killing of *E. coli* in Mϕ. (A) Mϕ from *Cybb*$^{-/-}$ *Nos2*$^{-/-}$ or WT littermate controls were infected with *S. aureus* at an MOI of 10. At 1 h after infection, the extracellular bacteria were removed by washing with PBS, followed by gentamicin treatment. At 2 h after infection, the cells were exposed to either normoxia (N) or hypoxia (H; 0.5% oxygen). For reoxygenation (Re), the cells were first incubated for 8 h under hypoxic conditions and then kept in normoxia. Cell lysates were prepared 2 and 24 h after infection to determine the amount of CFU inside the cells. The relative survival was calculated by dividing the amount of intracellular bacteria recovered 24 h after infection relative to the amount of intracellular bacteria determined 2 h after infection. The data are means + the SEM of at least four experiments. *, $P < 0.05$; **, $P < 0.01$; ***, $P < 0.001$. (B) Mϕ from *Cybb*$^{-/-}$ *Nos2*$^{-/-}$ or WT littermate controls were infected with *E. coli* as described in panel A. The data are means + the SEM of two experiments. *, $P < 0.05$; **, $P < 0.01$; ***, $P < 0.001$.

PHOX resulted in a decreased production of RNI and ROI (see Fig. S3 in the supplemental material). Second, *Cybb*$^{-/-}$ *Nos2*$^{-/-}$ and WT Mϕ did not differ in apoptosis or necrosis rates after infection with *E. coli* or *S. aureus* under normoxic conditions (see Fig. S4 in the supplemental material). Third, we analyzed whether an infection with *E. coli* or *S. aureus* or incubation under hypoxia affects the viability of *Cybb*$^{-/-}$ *Nos2*$^{-/-}$ and WT host cells. To this end, we measured the LDH activity in the culture supernatant and the lysates of infected Mϕ. Neither the infection nor the hypoxic culture condition significantly reduced the viability of WT or *Cybb*$^{-/-}$ *Nos2*$^{-/-}$ Mϕ (see Fig. S5 in the supplemental material).

Finally, we compared the ability of Mϕ from WT and *Cybb*$^{-/-}$ *Nos2*$^{-/-}$ mice to control an infection with *E. coli* or *S. aureus* under normoxic, hypoxic, or reoxygenated conditions. Normoxic *Cybb*$^{-/-}$ *Nos2*$^{-/-}$ Mϕ were impaired in their ability to clear *S. aureus* compared to normoxic WT cells (Fig. 5A). More importantly, however, the survival of *S. aureus* in hypoxic *Cybb*$^{-/-}$ *Nos2*$^{-/-}$ Mϕ was significantly higher than in normoxic *Cybb*$^{-/-}$ *Nos2*$^{-/-}$ cells and also clearly increased compared to hypoxic WT cells (Fig. 5A). These data indicate that, apart from PHOX and NOS2, an additional oxygen-dependent antimicrobial effector mechanism accounts for the killing of *S. aureus* by Mϕ, which becomes particularly evident in the absence of PHOX and NOS2.

Unlike the *S. aureus* infection model, *Cybb*$^{-/-}$ *Nos2*$^{-/-}$ Mϕ showed a reduced rather than an increased survival of *E. coli* under normoxic conditions compared to WT cells at the time point of analysis (24 h after infection) (Fig. 5B). Although we observed a limited NOS2/PHOX-dependent killing of *E. coli* at early time points of infection (up to 2 h [data not shown]), NOS2 and PHOX were clearly dispensable for the ultimate control of *E. coli* by Mϕ *in vitro*. During hypoxia the bacterial burden not only increased in *E. coli*-infected

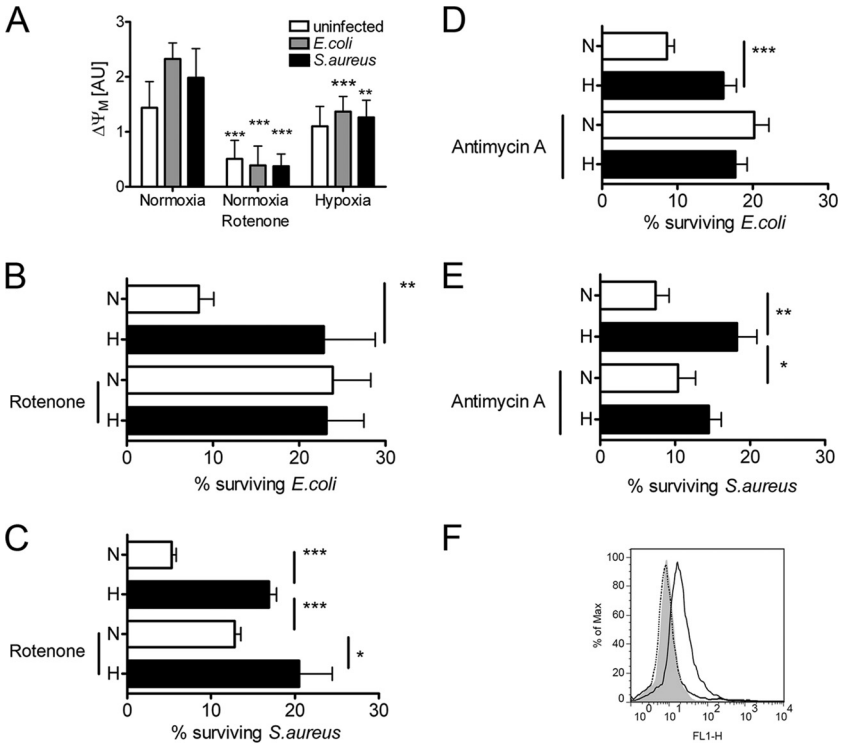

FIG 6 Hypoxia impairs mitochondrial activity in Mϕ, and inhibition of the mitochondrial respiratory chain completely or partially mimics the effect of hypoxia on the killing of *E. coli* or *S. aureus* by Mϕ, respectively. (A) Mϕ were infected with *E. coli* or *S. aureus* at an MOI of 10. At 1 h after infection, extracellular bacteria were removed by washing with PBS, followed by gentamicin treatment. At 2 h after infection, the cells were exposed to either normoxia (N) or hypoxia (H; 0.5% oxygen) in the absence or presence of rotenone (100 μM). After at least 24 h, the cells were stained with JC-1. The mitochondrial membrane potential ($\Delta\Psi_M$) was determined and is given in arbitrary units (AU). The data are means + the SD out of three similar experiments performed in triplicate. *, $P < 0.05$; **, $P < 0.01$; ***, $P < 0.001$. (B and C) Cells were infected with *E. coli* (B) or *S. aureus* (C) and treated as described in panel A. Cell lysates were prepared 2 and 24 h after infection to determine the number of CFU inside the cells. The relative survival was calculated by dividing the amount of intracellular bacteria recovered 24 h after infection related to the amount of intracellular bacteria determined 2 h after infection. The data are means + the SEM of six experiments. *, $P < 0.05$; **, $P < 0.01$; ***, $P < 0.001$. (D and E) Cells were infected with *E. coli* (D) or *S. aureus* (E). At 2 h after infection, the cells were exposed to either normoxia (N) or hypoxia (H; 0.5% oxygen) in the absence or presence of antimycin A (4 μg/ml). Cell lysates were prepared 2 and 24 h after infection to determine the number of CFU inside the cells. The relative survival was calculated by dividing the amount of intracellular bacteria recovered 24 h after infection related to the amount of intracellular bacteria determined 2 h after infection. The data are means + the SEM of at least four experiments. *, $P < 0.05$; **, $P < 0.01$; ***, $P < 0.001$. (F) Mϕ were left untreated or treated with rotenone (100 μM) and subjected to normoxic or hypoxic conditions. After 24 h, the cells were labeled with CM-H_2DCFDA, fixed with 3.5% PFA, and analyzed by flow cytometry. The gray-shaded curve indicates the FL-1 fluorescence of labeled cells under normoxic conditions. The black dotted curve indicates the FL-1 fluorescence of CM-H_2DCFDA-labeled cells after stimulation with rotenone and incubation under hypoxic conditions, and the black solid curve demonstrates the FL-1 fluorescence of CM-H_2DCFDA-labeled cells after stimulation with rotenone and incubation under normoxic conditions.

WT Mϕ but also in *Cybb*$^{-/-}$ *Nos2*$^{-/-}$ Mϕ (Fig. 5B). From these data, we conclude that the control of *E. coli* by Mϕ is due to a PHOX- and NOS2-independent, but oxygen-dependent effector mechanism.

Hypoxia inhibits the activity of the mitochondrial respiratory chain in *E. coli*- or *S. aureus*-infected Mϕ. Mitochondrial activity is impaired under hypoxia (14). Sonoda et al. demonstrated that Mϕ that are genetically defective for mitochondrial ROI production show a decreased capacity to degrade intracellular *L. monocytogenes* compared to WT Mϕ, even in the presence of an inhibitor of NOS2 or PHOX (78). In order to determine the mitochondrial activity of infected Mϕ, we determined the mitochondrial membrane potential ($\Delta\Psi_M$) by using JC-1 dye. The lipophilic, cationic dye JC-1 can selectively enter into mitochondria and reversibly change color from green to red as the membrane potential increases. In cells with a high $\Delta\Psi_M$, JC-1 spontaneously forms complexes known as J-aggregates with intense red fluorescence. In cells with a low $\Delta\Psi_M$, JC-1 remains in the monomeric form, which shows only green fluorescence. The ratio of this red/green fluorescence is independent of mitochondrial shape, density, or size but depends only on the membrane potential (15). Since this dye is not suitable for fixation, we sealed the plates harboring the infected cells with an adhesive clear seal suitable for qRT-PCR applications in order to preserve the respective normoxic and hypoxic condition. We observed that in infected Mϕ the $\Delta\Psi_M$ decreased in rotenone- and hypoxia-treated cells (Fig. 6A). However, the hypoxic impairment of $\Delta\Psi_M$ was not due to toxic effects because within 5 min of reoxygenation (i.e., removal of the adhesive seal), we observed a substantial increase of $\Delta\Psi_M$ in *S. aureus*-infected (data not shown) and *E. coli*-infected (see Fig. S6 in the supplemental material) Mϕ. Thus, we conclude that hypoxia works in analogy to rotenone and interferes with mitochondrial activity.

Inhibition of the mitochondrial respiratory chain completely or partially mimics the effect of hypoxia on the killing of *E. coli* and *S. aureus*, respectively. Next, we analyzed the fate of *E. coli* in Mϕ after inhibition of mitochondrial respiration. For that purpose, we used rotenone that binds to the ubiquinone binding site of complex I and thereby interferes with electron transport. We used different concentrations of rotenone (10 μM, 100 μM, and 1 mM) and correlated this treatment with the bactericidal

activity of *E. coli*-infected Mϕ. Rotenone at 10 μM barely inhibited the bactericidal activity. However, 100 μM rotenone robustly impaired the antibacterial capacity (see Fig. S7 in the supplemental material). Rotenone at 1 mM appeared to be toxic to the host cells. For further experiments, we therefore used a 100 μM concentration, which proved to sufficiently inhibit mitochondrial activity (Fig. 6A). For the control of host cell viability, we analyzed the relative LDH release rate and NO production under normoxic and hypoxic conditions in the absence or presence of rotenone. At the concentrations used we could not detect any toxicity of rotenone in LDH release assays (see Fig. S5 in the supplemental material). Moreover, inhibition of mitochondrial respiration did not affect NO production upon infection (see Fig. S8 in the supplemental material). In order to exclude that rotenone inhibits bacterial cell division and viability *in vitro*, we analyzed the growth of *E. coli* in the absence or presence of rotenone. We found that *E. coli* grew equally well in the presence or absence of rotenone (see Fig. S9 in the supplemental material) as described previously (27). When rotenone was added to *E. coli*-infected Mϕ under normoxic conditions, we found that the bacterial survival rate exactly reached the level observed in hypoxic Mϕ without rotenone. Importantly, the addition of rotenone to hypoxic cultures did not further inhibit the antimicrobial activity of Mϕ (Fig. 6B). However, treatment of *S. aureus*-infected WT Mϕ with rotenone under normoxic conditions did not lead to the same increase of *S. aureus*, as seen in hypoxic Mϕ cultures in the absence of rotenone (Fig. 6C).

Furthermore, we used antimycin A to inhibit the coenzyme Q/cytochrome *c*/oxidoreductase, which is located in complex III of the respiratory chain. Antimycin A did not interfere with bacterial cell division and viability *in vitro* (see Fig. S11 in the supplemental material). After treatment of *E. coli*-infected macrophages with antimycin A, bacterial survival reached exactly the level of hypoxia-treated macrophages (Fig. 6D). However, treatment of *S. aureus*-infected WT Mϕ with antimycin A did not lead to the same increase of *S. aureus* as seen in hypoxic Mϕ cultures in the absence of antimycin A (Fig. 6E). Therefore, we conclude that inhibition of mitochondrial activity completely or partially mimicked the defective antibacterial capacity observed in hypoxic *E. coli*- or *S. aureus*-infected WT Mϕ.

Inhibition of the mitochondrial respiratory chain and not mitochondrial ROI account for rotenone's effects on bactericidal activity. Next, we wanted to clarify whether mitochondrial respiration or mitochondrial ROI accounts for our observation. In accordance with the findings from West et al. (84), we observed an increased production of ROI after treatment of Mϕ with rotenone under normoxic conditions (Fig. 6F). However, we did not observe a significant ROI production of Mϕ infected with *E. coli* or *S. aureus* under hypoxic conditions (see Fig. S3 in the supplemental material; Fig. 4C). Thus, treatment of macrophages with rotenone and hypoxic treatment led to a change in ROI levels in opposite directions. Since hypoxia and rotenone induced similar effects on the mitochondrial and bactericidal killing, we conclude that mitochondrial respiration and not mitochondrial ROI accounts for our findings.

Inhibition of the mitochondrial respiratory chain is the PHOX- and NOS2-independent component of the impaired killing of *S. aureus* by Mϕ during hypoxia. Having seen that a lack of PHOX and NOS2 activity only partially explains the reduced antibacterial activity of Mϕ against *S. aureus* during hypoxia (Fig. 5), we performed the reverse experimental approach and tested the effect of inhibition of mitochondrial respiratory chain activity on the survival of *S. aureus*. Treatment of *S. aureus*-infected WT Mϕ with rotenone under normoxic conditions did not lead to the same increase of *S. aureus*, as seen in hypoxic Mϕ cultures in the absence of rotenone. Furthermore, exposure of *S. aureus*-infected WT Mϕ to rotenone during hypoxia caused an additional significant increase in the bacterial load compared to the normoxic or rotenone-free hypoxic controls (Fig. 7). In *Cybb*$^{-/-}$ *Nos2*$^{-/-}$ Mϕ cultures rotenone treatment raised the bacterial numbers by a factor of 2.5 during normoxia but was ineffective under hypoxic conditions. These data demonstrate that PHOX and NOS2, as well as an oxygen-dependent mitochondrial antibacterial killing mechanism, contribute to the control of *S. aureus* in Mϕ.

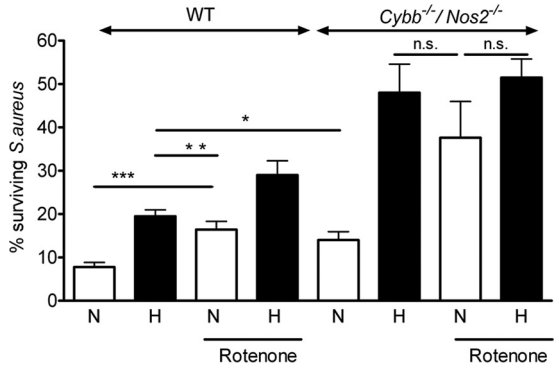

FIG 7 Inhibition of the mitochondrial respiratory chain is the PHOX- and NOS2-independent component of the impaired killing of *S. aureus* by Mϕ during hypoxia. Mϕ from *Cybb*$^{-/-}$ *Nos2*$^{-/-}$ or WT littermate controls were infected with *S. aureus.* At 1 h after infection, extracellular bacteria were removed by washing with PBS, followed by gentamicin treatment. At 2 h after infection, the cells were exposed to either normoxia (N) or hypoxia (H; 0.5% oxygen) in the absence or presence of rotenone (100 μM). Cell lysates were prepared 2 and 24 h after infection to determine the amount of CFU inside the cells. The relative survival was calculated by dividing the amount of intracellular bacteria recovered 24 h after infection relative to the amount of intracellular bacteria determined 2 h after infection. The data are means + the SEM of at least four experiments. *, $P < 0.05$; **, $P < 0.01$; ***, $P < 0.001$.

DISCUSSION

To the best of our knowledge, the present study demonstrates for the first time that hypoxia impairs the bactericidal activity of primary Mϕ. A related observation has previously been made with human neutrophils, which turned out to be poor killers of *E. coli* and *S. aureus* under anaerobic conditions (49). McGovern et al. attributed this reduced killing of granulocytes to an inhibition of the PHOX-dependent respiratory burst (51). Our present data obtained with primary Mϕ illustrate that, in addition to PHOX and NOS2, the mitochondrial respiratory chain is highly relevant for the antibacterial activity of phagocytes. Collectively, these *in vitro* observations with myeloid cells offer an explanation for the aggravated course of *S. aureus* lung and skin infections following systemic hypoxia *in vivo* (29, 30, 38). Interestingly, hypoxia—a milieu often encountered in estuarine marine habitats—also inhibits the elimination of *Vibrio campbellii* in the economically important shellfish species *Crassostera virginica* (48). This indicates that oxygen availability is of general importance for the control of bacterial pathogens by host organisms.

Hypoxia and antibacterial activity. It is important to emphasize that hypoxia does not uniformly impair the control of all bacteria by host cells. Infection of Hep-2 cells with *C. pneumoniae* under hypoxic conditions supported the recovery of infectious elementary bodies from these cells (68). Unlike infections with *E. coli* and *S. aureus*, hypoxia did not impede the killing of *Staphylococcus epidermidis*, viridans streptococci, or enterococci in neutrophils or Mϕ (49, 60), which clearly points to a critical role of oxygen-independent antimicrobial mechanisms such as the cationic bactericidal/permeability-increasing protein of neutrophils (24, 82). Our data also show that a large portion of the entire inoculum of *E. coli* and *S. aureus* was killed even under hypoxic conditions, which underscores the existence of oxygen-independent mechanisms also in Mϕ. However, the available data and our work do not support Paul Ehrlich's general assumption that hypoxia *per se* promotes the antibacterial capacity of host cells (22). Therefore, we conclude that tissue oxygenation is an important environmental factor that enables the innate immune system to sweep off invading bacteria.

Hypoxia and the role of HIF-α for bacterial killing. The results of the present study demonstrate that the impaired antimicrobial capacity is not causally related to the enhanced HIF1A activity observed under hypoxic conditions. This finding contrasts with two previous reports on the role of HIF1A in bacterial infections (16, 60). However, several experimental differences may account for the divergent results. First, in these earlier studies HIF1A-deficient Mϕ were used; details on the genetic background of these mice were not given. Second, the killing assays were performed with group A or B streptococci and *Pseudomonas aeruginosa* rather than *E. coli* and *S. aureus* and were restricted to 2-h infection time points. Third, a 4-fold-lower MOI (i.e., 2.5) for streptococci and a 2.5-fold-higher MOI (i.e., 25) for *P. aeruginosa* were used (16, 60). That details of the experimental setup can have a striking influence on the role of HIF1A in bacterial infections is further supported by the fact that a pharmacological upregulation of HIF1A activity boosted the bactericidal capacity in a mouse skin infection model with *S. aureus* (86), whereas HIF1A inhibition after induction of a *S. aureus* peritonitis ameliorated the outcome of this infection (83).

Intriguingly, compared to hypoxic stimulation, the infection of Mϕ with *E. coli* and *S. aureus* under normoxic conditions resulted in a very robust accumulation of HIF2A. This suggests that HIF2A may play an important role in the bactericidal activity of myeloid cells. This is supported by recent data showing that HIF2A regulates the inflammatory activity of macrophages (33). To date, there is no information on a possible antimicrobial effect of HIF2A in macrophages. Further studies are needed to address this issue.

Role PHOX and NOS2 for the killing of bacteria. Prior to the present study, it was fair to assume that *Cybb*$^{-/-}$ *Nos2*$^{-/-}$ myeloid cells will replicate the phenotype of reduced bacterial killing under hypoxic conditions based on the oxygen dependency of PHOX and NOS2. Indeed, oxygen deprivation was demonstrated to inhibit the activity of both NOS2 and PHOX (2, 18, 41, 44, 51, 66, 81). Furthermore, it was shown that *Cybb*$^{-/-}$ *Nos2*$^{-/-}$ peritoneal exudate Mϕ have an impaired antibacterial capacity, as assessed 4 h after infection with *E. coli* HB101. This reduced *in vitro* killing capacity correlated with the occurrence of spontaneous *E. coli* abscesses in *Cybb*$^{-/-}$ *Nos2*$^{-/-}$ mice (75). In our study, in contrast, normoxic *Cybb*$^{-/-}$ *Nos2*$^{-/-}$ Mϕ were even more potent than Mϕ from WT littermates in killing *E. coli*, as determined 24 h after infection (Fig. 5B). A time course analysis, however, revealed an impaired killing of *E. coli* by *Cybb*$^{-/-}$ *Nos2*$^{-/-}$ Mϕ within the first 2 h after infection, which was no longer detectable at later time points (data not shown). Considering that the PHOX-dependent respiratory burst reaches its maximum within 30 min of stimulation (19, 80) and that *E. coli* exhibits various mechanisms of resistance to ROI and RNI (10, 50, 51, 64), it appears obvious that the ultimate control of *E. coli* by Mϕ is PHOX and NOS2 independent. Also, as the exposure to hypoxia was only started at 2 h after infection in our experimental setting (see Fig. 1), it follows that the increased survival of *E. coli* in Mϕ during hypoxia results from the defect of an oxygen-dependent, but PHOX- and NOS2-independent antimicrobial effector mechanism.

S. aureus effectively triggers PHOX activity (73) and, depending on the context, is a potent inducer of NOS2 (17). *In vivo*, mice deficient for either PHOX or NOS2 have an increased susceptibility to *S. aureus* infections (52, 69, 70). Macrophages from mice with an individual knockout of the PHOX or NOS2 gene showed an unaltered ability to kill *S. aureus in vitro* compared to WT Mϕ (42), whereas neutrophils from PHOX-deficient mice were ineffective in killing *S. aureus* (23, 34, 62). Our present data with *Cybb*$^{-/-}$ *Nos2*$^{-/-}$ double-deficient Mϕ demonstrate that *S. aureus* is partially controlled by PHOX and NOS2. However, in hypoxic WT Mϕ the killing of *S. aureus* was more severely impaired than in normoxic *Cybb*$^{-/-}$ *Nos2*$^{-/-}$ Mϕ. This strongly argues for the operation of an oxygen-dependent, PHOX/NOS2-independent mechanism, as already seen in *E. coli*-infected Mϕ.

Antibacterial effector function of mitochondria. In the present study the mitochondrial respiratory chain contributed to the antimicrobial activity of Mϕ to a different extent depending on the microbial species (*E. coli* versus *S. aureus*). Its antimicrobial role was unambiguously documented by the use of inhibitors of mitochondrial respiration, which in normoxic WT Mϕ infected with *E. coli* or *Cybb*$^{-/-}$ *Nos2*$^{-/-}$ Mϕ infected with *S. aureus* mimicked the respective hypoxia phenotype. This finding is entirely in line with the observation that hypoxia inhibits the function of mitochondria, notably mitochondrial complex I activity, which involves a miR-210-mediated repression of iron-sulfur enzymes (14). Earlier studies had already suggested that the mitochondrial respiratory chain and/or mitochondrial ROI participate in the defense against *Listeria monocytogenes* or *Toxoplasma gondii* (4, 67, 78). Most recently, West et al. described yet another facet to the role of mitochondria in antibacterial defense. They were able to demonstrate that the activation of Mϕ by TLR ligands leads to the recruitment of mitochondria toward the phagosome and to the augmentation of mitochondrial ROI production. Inhibition of this process by deletion of required adaptor molecules impaired the killing of intracellular *Salmonella* (84). Our present work extends these findings by demonstrating that in Mϕ from normal WT mice a functional mitochondrial respiratory chain is crucial for full antimicrobial activity, as demonstrated by the effects of hypoxia and rotenone.

Together, these findings shed new light on the role of mitochondria in myeloid cells. Already at the beginning of the 20th century several studies documented that myeloid cells are highly dependent on aerobic glycolysis for energy generation and function (6, 16, 28, 46, 72), whereas an inhibition of mitochondrial activity failed to influence their energy generation (11, 57). Accordingly, neither gamma interferon nor LPS stimulation pro-

moted fatty acid β-oxidation (43, 78) but instead increased mitochondrial ROI production in Mϕ (25, 78). This strongly suggests that mitochondrial function may be beyond energy generation. We propose that in the presence of ample oxygen myeloid cells can utilize mitochondria for antimicrobial defense because they can shift the energy generation from mitochondria to aerobic glycolysis resembling a metabolic process induced in transformed cells ("Warburg effect").

There are at least two clinical situations in which an impaired mitochondrial activity in Mϕ may account for the occurrence of severe infections. First, the Barth syndrome, a rare X-linked recessive disorder, is associated with mitochondrial dysfunction. Cardiac failure and septicemia are the leading causes of death of children suffering from this disease (7). Until now neutropenia has been considered as the main factor predisposing these patients to septicemia. However, mitochondrial dysfunction of Mϕ and hence a reduced bactericidal activity may very well contribute to the fatal infections. Second, mitochondrial damage has been associated with poor outcome in sepsis patients (26). Mitochondrial dysfunction may be a consequence of hypoxia and hypoxic signaling, which is commonly encountered in the tissues of septic patients, or induced by pathogens, their products, and/or inflammatory mediators. It is tempting to speculate that the predisposition of septic patients to opportunistic infections in intensive care units may be associated with the dysfunction of mitochondria in mononuclear phagocytes, which normally keep commensal bacteria at bay.

In summary, hypoxia shuts down not only the enzyme activity of PHOX and NOS2 but also the antibacterial effector function of mitochondria. Further studies are needed to precisely investigate the mechanisms by which mitochondria promote oxygen-dependent bacterial clearance and to determine how hypoxia interferes with that process in mononuclear phagocytes.

ACKNOWLEDGMENTS

We thank Anja Lührmann for stimulating discussions.

This study was supported by grants to C.B., M.H., and J.J. from the Deutsche Forschungsgemeinschaft (Bo996/3-3, SFB643 project A6, JA 1993/1-1), by grants to C.B., M.H., C.W., and J.J. from the Interdisziplinäres Zentrum für Klinische Forschung (projects A24, A28, and A49), and by a grant to J.J. from the ELAN program (Az. 11.01.26.1) at the Universitätsklinikum Erlangen and Friedrich-Alexander-Universität Erlangen-Nürnberg.

REFERENCES

1. **Ackermann M, et al.** 2008. Self-destructive cooperation mediated by phenotypic noise. Nature **454**:987–990.
2. **Albina JE, Henry WL, Jr, Mastrofrancesco B, Martin BA, Reichner JS.** 1995. Macrophage activation by culture in an anoxic environment. J. Immunol. **155**:4391–4396.
3. **Anand RJ, et al.** 2007. Hypoxia causes an increase in phagocytosis by macrophages in a HIF-1α-dependent manner. J. Leukoc. Biol. **82**:1257–1265.
4. **Arsenijevic D, et al.** 2000. Disruption of the uncoupling protein-2 gene in mice reveals a role in immunity and reactive oxygen species production. Nat. Genet. **26**:435–439.
5. **Atkuri KR, Herzenberg LA, Niemi AK, Cowan T, Herzenberg LA.** 2007. Importance of culturing primary lymphocytes at physiological oxygen levels. Proc. Natl. Acad. Sci. U. S. A. **104**:4547–4552.
6. **Bakker A.** 1927. Einige Übereinstimmungen im Stoffwechsel der Carcinomzellen und Exsudatleukocyten. Klin. Wochenschr. **6**:252.
7. **Barth PG, et al.** 1999. X-linked cardioskeletal myopathy and neutropenia (Barth syndrome) (MIM 302060). J. Inherit. Metab. Dis. **22**:555–567.
8. **Bogdan C.** 2011. Reactive oxygen and reactive nitrogen intermediates in the immune system, p 69–84. *In* Kaufmann SH, Rouse B, Sacks D (ed), Immunology of infectious diseases. ASM Press, Washington, DC.
9. **Bogdan C, Rollinghoff M, Diefenbach A.** 2000. Reactive oxygen and reactive nitrogen intermediates in innate and specific immunity. Curr. Opin. Immunol. **12**:64–76.
10. **Bonamore A, Boffi A.** 2008. Flavohemoglobin: structure and reactivity. IUBMB Life **60**:19–28.
11. **Borregaard N, Herlin T.** 1982. Energy metabolism of human neutrophils during phagocytosis. J. Clin. Invest. **70**:550–557.
12. **Caldwell CC, et al.** 2001. Differential effects of physiologically relevant hypoxic conditions on T lymphocyte development and effector functions. J. Immunol. **167**:6140–6149.
13. **Campbell JA.** 1925. The influence of O_2 tension in the inspired air upon the O_2 tension in the tissues. J. Physiol. **60**:20–29.
14. **Chan SY, et al.** 2009. MicroRNA-210 controls mitochondrial metabolism during hypoxia by repressing the iron-sulfur cluster assembly proteins ISCU1/2. Cell Metab. **10**:273–284.
15. **Chazotte B.** September 2011. Labeling mitochondria with JC-1. Cold Spring Harbor Protoc. doi:10.1101/pdb.prot065490.
16. **Cramer T, et al.** 2003. HIF-1α is essential for myeloid cell-mediated inflammation. Cell **112**:645–657.
17. **Cunha FQ, Assreuy J, Moncada S, Liew FY.** 1993. Phagocytosis and induction of nitric oxide synthase in murine macrophages. Immunology **79**:408–411.
18. **Daniliuc S, et al.** 2003. Hypoxia inactivates inducible nitric oxide synthase in mouse macrophages by disrupting its interaction with alpha-actinin 4. J. Immunol. **171**:3225–3232.
19. **De la Harpe J, Nathan CF.** 1985. A semi-automated micro-assay for H2O2 release by human blood monocytes and mouse peritoneal macrophages. J. Immunol. Methods **78**:323–336.
20. **Ding AH, Nathan CF, Stuehr DJ.** 1988. Release of reactive nitrogen intermediates and reactive oxygen intermediates from mouse peritoneal macrophages: comparison of activating cytokines and evidence for independent production. J. Immunol. **141**:2407–2412.
21. **Dlaska M, Weiss G.** 1999. Central role of transcription factor NF-IL6 for cytokine and iron-mediated regulation of murine inducible nitric oxide synthase expression. J. Immunol. **162**:6171–6177.
22. **Ehrlich P.** 1885. Das Sauerstoff-Bedürfniss des Organismus, vol 1. Springer-Verlag, Berlin, Germany.
23. **Ellson CD, et al.** 2006. Neutrophils from *p40phox*$^{-/-}$ mice exhibit severe defects in NADPH oxidase regulation and oxidant-dependent bacterial killing. J. Exp. Med. **203**:1927–1937.
24. **Elsbach P, Weiss J.** 1985. Oxygen-dependent and oxygen-independent mechanisms of microbicidal activity of neutrophils. Immunol. Lett. **11**:159–163.
25. **Emre Y, et al.** 2007. Mitochondria contribute to LPS-induced MAPK activation via uncoupling protein UCP2 in macrophages. Biochem. J. **402**:271–278.
26. **Exline MC, Crouser ED.** 2008. Mitochondrial mechanisms of sepsis-induced organ failure. Front. Biosci. **13**:5030–5041.
27. **Finel M.** 1996. Genetic inactivation of the H^+-translocating NADH: ubiquinone oxidoreductase of *Paracoccus denitrificans* is facilitated by insertion of the *ndh* gene from *Escherichia coli*. FEBS Lett. **393**:81–85.
28. **Fleischmann W, Kubowitz F.** 1927. Über den Stoffwechsel der Leukocyten. Biochem. Z. **181**:395.
29. **Green GM, Kass EH.** 1964. Factors influencing the clearance of bacteria by the lung. J. Clin. Invest. **43**:769–776.
30. **Harris GD, Johanson WG, Jr, Pierce AK.** 1977. Determinants of lung bacterial clearance in mice after acute hypoxia. Am. Rev. Respir. Dis. **116**:671–677.
31. **Helaine S, et al.** 2010. Dynamics of intracellular bacterial replication at the single cell level. Proc. Natl. Acad. Sci. U. S. A. **107**:3746–3751.
32. **Hunt TK, Twomey P, Zederfeldt B, Dunphy JE.** 1967. Respiratory gas tensions and pH in healing wounds. Am. J. Surg. **114**:302–307.
33. **Imtiyaz HZ, et al.** 2010. Hypoxia-inducible factor 2alpha regulates macrophage function in mouse models of acute and tumor inflammation. J. Clin. Invest. **120**:2699–2714.
34. **Jackson SH, Gallin JI, Holland SM.** 1995. The p47phox mouse knockout model of chronic granulomatous disease. J. Exp. Med. **182**:751–758.
35. **Jantsch J, et al.** 2008. Hypoxia and hypoxia-inducible factor-1 alpha modulate lipopolysaccharide-induced dendritic cell activation and function. J. Immunol. **180**:4697–4705.
36. **Jantsch J, et al.** 2008. Small interfering RNA (siRNA) delivery into murine

bone marrow-derived dendritic cells by electroporation. J. Immunol. Methods **337**:71–77.
37. **Jantsch J, et al.** Toll-like receptor activation and hypoxia use distinct signaling pathways to stabilize hypoxia-inducible factor 1α (HIF1A) and result in differential HIF1A-dependent gene expression. J. Leukoc. Biol. **90**:551–562.
38. **Jonsson K, Hunt TK, Mathes SJ.** 1988. Oxygen as an isolated variable influences resistance to infection. Ann. Surg. **208**:783–787.
39. **Kaelin WG, Jr, Ratcliffe PJ.** 2008. Oxygen sensing by metazoans: the central role of the HIF hydroxylase pathway. Mol. Cell **30**:393–402.
40. **Karhausen J, et al.** 2004. Epithelial hypoxia-inducible factor-1 is protective in murine experimental colitis. J. Clin. Invest. **114**:1098–1106.
41. **Kim N, et al.** 1993. Oxygen tension regulates the nitric oxide pathway: physiological role in penile erection. J. Clin. Invest. **91**:437–442.
42. **Kohler J, et al.** NADPH-oxidase but not inducible nitric oxide synthase contributes to resistance in a murine *Staphylococcus aureus* Newman pneumonia model. Microbes Infect. **13**:914–922.
43. **Krawczyk CM, et al.** 2010. Toll-like receptor-induced changes in glycolytic metabolism regulate dendritic cell activation. Blood **115**:4742–4749.
44. **Kwon NS, et al.** 1990. L-Citrulline production from L-arginine by macrophage nitric oxide synthase: the ureido oxygen derives from dioxygen. J. Biol. Chem. **265**:13442–13445.
45. **Laser H.** 1937. Tissue metabolism under the influence of low oxygen tension. Biochem. J. **31**:1671–1676.
46. **Levene PA, Meyer GM.** 1912. The action of leucocytes on glucose, second communication. J. Biol. Chem. **12**:265–273.
47. **Lissner CR, Weinstein DL, O'Brien AD.** 1985. Mouse chromosome 1 *Ity* locus regulates microbicidal activity of isolated peritoneal macrophages against a diverse group of intracellular and extracellular bacteria. J. Immunol. **135**:544–547.
48. **Macey BM, Achilihu IO, Burnett KG, Burnett LE.** 2008. Effects of hypercapnic hypoxia on inactivation and elimination of *Vibrio campbellii* in the Eastern oyster, *Crassostrea virginica*. Appl. Environ. Microbiol. **74**: 6077–6084.
49. **Mandell GL.** 1974. Bactericidal activity of aerobic and anaerobic polymorphonuclear neutrophils. Infect. Immun. **9**:337–341.
50. **Mason MG, et al.** 2009. Cytochrome bd confers nitric oxide resistance to *Escherichia coli*. Nat. Chem. Biol. **5**:94–96.
51. **McGovern NN, et al.** Hypoxia selectively inhibits respiratory burst activity and killing of *Staphylococcus aureus* in human neutrophils. J. Immunol. **186**:453–463.
52. **McInnes IB, Leung B, Wei XQ, Gemmell CC, Liew FY.** 1998. Septic arthritis following *Staphylococcus aureus* infection in mice lacking inducible nitric oxide synthase. J. Immunol. **160**:308–315.
53. **Melillo G, et al.** 1997. Functional requirement of the hypoxia-responsive element in the activation of the inducible nitric oxide synthase promoter by the iron chelator desferrioxamine. J. Biol. Chem. **272**:12236–12243.
54. **Mi Z, et al.** 2008. Synergystic induction of HIF-1α transcriptional activity by hypoxia and lipopolysaccharide in macrophages. Cell Cycle **7**:232–241.
55. **Nangaku M, Eckardt KU.** 2007. Hypoxia and the HIF system in kidney disease. J. Mol. Med. **85**:1325–1330.
56. **Niinikoski J, Grislis G, Hunt TK.** 1972. Respiratory gas tensions and collagen in infected wounds. Ann. Surg. **175**:588–593.
57. **O'Flaherty JT, Kreutzer DL, Showell HJ, Ward PA.** 1977. Influence of inhibitors of cellular function on chemotactic factor-induced neutrophil aggregation. J. Immunol. **119**:1751–1756.
58. **Peyssonnaux C, et al.** 2008. Critical role of HIF-1α in keratinocyte defense against bacterial infection. J. Invest. Dermatol. **128**:1964–1968.
59. **Peyssonnaux C, et al.** 2007. Cutting edge: essential role of hypoxia inducible factor-1α in development of lipopolysaccharide-induced sepsis. J. Immunol. **178**:7516–7519.
60. **Peyssonnaux C, et al.** 2005. HIF-1α expression regulates the bactericidal capacity of phagocytes. J. Clin. Invest. **115**:1806–1815.
61. **Pfeifer JD, Wick MJ, Russell DG, Normark SJ, Harding CV.** 1992. Recombinant *Escherichia coli* express a defined, cytoplasmic epitope that is efficiently processed in macrophage phagolysosomes for class II MHC presentation to T lymphocytes. J. Immunol. **149**:2576–2584.
62. **Pollock JD, et al.** 1995. Mouse model of X-linked chronic granulomatous disease, an inherited defect in phagocyte superoxide production. Nat. Genet. **9**:202–209.
63. **Pouyssegur J, Dayan F, Mazure NM.** 2006. Hypoxia signalling in cancer and approaches to enforce tumour regression. Nature **441**:437–443.
64. **Rada BK, Geiszt M, Kaldi K, Timar C, Ligeti E.** 2004. Dual role of phagocytic NADPH oxidase in bacterial killing. Blood **104**:2947–2953.
65. **Remensnyder JP, Majno G.** 1968. Oxygen gradients in healing wounds. Am. J. Pathol. **52**:301–323.
66. **Robinson MA, Baumgardner JE, Good VP, Otto CM.** 2008. Physiological and hypoxic O_2 tensions rapidly regulate NO production by stimulated macrophages. Am. J. Physiol. **294**:C1079–C1087.
67. **Rousset S, et al.** 2006. The uncoupling protein 2 modulates the cytokine balance in innate immunity. Cytokine **35**:135–142.
68. **Rupp J, et al.** 2007. *Chlamydia pneumoniae* directly interferes with HIF-1α stabilization in human host cells. Cell Microbiol. **9**:2181–2191.
69. **Sakiniene E, Bremell T, Tarkowski A.** 1997. Inhibition of nitric oxide synthase (NOS) aggravates *Staphylococcus aureus* septicemia and septic arthritis. Clin. Exp. Immunol. **110**:370–377.
70. **Sasaki S, et al.** 1998. Protective role of nitric oxide in *Staphylococcus aureus* infection in mice. Infect. Immun. **66**:1017–1022.
71. **Sawyer RG, Spengler MD, Adams RB, Pruett TL.** 1991. The peritoneal environment during infection: the effect of monomicrobial and polymicrobial bacteria on pO_2 and pH. Ann. Surg. **213**:253–260.
72. **Sbarra AJ, Karnovsky ML.** 1959. The biochemical basis of phagocytosis. I. Metabolic changes during the ingestion of particles by polymorphonuclear leukocytes. J. Biol. Chem. **234**:1355–1362.
73. **Segal AW, Geisow M, Garcia R, Harper A, Miller R.** 1981. The respiratory burst of phagocytic cells is associated with a rise in vacuolar pH. Nature **290**:406–409.
74. **Semenza GL.** 2010. Defining the role of hypoxia-inducible factor 1 in cancer biology and therapeutics. Oncogene **29**:625–634.
75. **Shiloh MU, et al.** 1999. Phenotype of mice and macrophages deficient in both phagocyte oxidase and inducible nitric oxide synthase. Immunity **10**:29–38.
76. **Shohet RV, Garcia JA.** 2007. Keeping the engine primed: HIF factors as key regulators of cardiac metabolism and angiogenesis during ischemia. J. Mol. Med. **85**:1309–1315.
77. **Sitkovsky M, Lukashev D.** 2005. Regulation of immune cells by local-tissue oxygen tension: HIF1α and adenosine receptors. Nat. Rev. Immunol. **5**:712–721.
78. **Sonoda J, et al.** 2007. Nuclear receptor ERRα and coactivator PGC-1β are effectors of IFN-γ-induced host defense. Genes Dev. **21**:1909–1920.
79. **Takeda N, et al.** 2010. Differential activation and antagonistic function of HIF-α isoforms in macrophages are essential for NO homeostasis. Genes Dev. **24**:491–501.
80. **VanderVen BC, Yates RM, Russell DG.** 2009. Intraphagosomal measurement of the magnitude and duration of the oxidative burst. Traffic **10**: 372–378.
81. **Wang JF, Komarov P, Sies H, de Groot H.** 1992. Inhibition of superoxide and nitric oxide release and protection from reoxygenation injury by Ebselen in rat Kupffer cells. Hepatology **15**:1112–1116.
82. **Weiss J, Victor M, Stendhal O, Elsbach P.** 1982. Killing of gram-negative bacteria by polymorphonuclear leukocytes: role of an O_2-independent bactericidal system. J. Clin. Invest. **69**:959–970.
83. **Werth N, et al.** 2010. Activation of hypoxia inducible factor 1 is a general phenomenon in infections with human pathogens. PLoS One **5**:e11576.
84. **West AP, et al.** TLR signalling augments macrophage bactericidal activity through mitochondrial ROS. Nature 472:476–480.
85. **Wiese M, et al.** 2010. Small interfering RNA (siRNA) delivery into murine bone marrow-derived macrophages by electroporation. J. Immunol. Methods **353**:102–110.
86. **Zinkernagel AS, Peyssonnaux C, Johnson RS, Nizet V.** 2008. Pharmacologic augmentation of hypoxia-inducible factor-1α with mimosine boosts the bactericidal capacity of phagocytes. J. Infect. Dis. **197**:214–217.